

## The crystal structure of monoclinic britholite-(Ce) and britholite-(Y)

David C. Noe, John M. Hughes

Department of Geology, Miami University, Oxford, OH 45056 USA

Anthony N. Mariano

48 Page Brook Road, Carlisle, MA 01741 USA

John W. Drexler

Department of Geological Sciences, University of Colorado, Boulder, CO 80309 USA

and Akira Kato

National Science Museum, Department of Geology, 3-23-1 Hyakunin-Cho,  
Shinjuku-Ku, Tokyo 169, Japan

Received: July 16, 1992

***Britholite-(Ce) | Britholite-(Y) | Crystal structure | Apatite analogues***

**Abstract.** The crystal structures of the monoclinic dimorphs of natural britholite-(Ce) and britholite-(Y) have been solved in space group  $P2_1$  using both annealed and unannealed samples. Like the  $P6_3$  britholite atomic arrangement reported recently, the structure of monoclinic britholite is similar to the apatite atomic arrangement.

The monoclinic britholite dimorph differs from its hexagonal counterpart principally in the ligation of the REE equivalent of the apatite Ca(1) site. Whereas in  $P6_3$  britholite each Ca(1) equivalent has either three short or three long REE-O(3) bonds, in the  $P2_1$  dimorph the Ca(1) equivalents have either one long and two short REE-O(3) bonds or one short and two long REE-O(3) bonds. Thus  $3/m$  is removed from the  $P6_3/m$  apatite symmetry elements, yielding  $P2_1$  symmetry. The symmetry reduction explains the common observation of biaxial optical characteristics of britholite samples.

## Introduction

Britholite is one of the more common and economically-important rare earth element (REE) bearing minerals, but considerable ambiguity has surrounded previous investigations of the phase. Britholite was first described (Winther, 1901) as an orthorhombic mineral that appeared pseudohexagonal by twinning on {110}. Some researchers (Winther, 1901; Hughes, Mariano, Drexler, 1992) have reported biaxial optical characteristics for the phase, whereas others (Bøggild, 1911; Hata, 1938; Hughson and Gupta, 1964; Genkina, Malinovskii, Khomyakov, 1991) have reported uniaxial optics. Two studies (Gay, 1957; Kupriyanova and Sidorenko, 1963) suggested that britholite can be *either* biaxial or uniaxial.

In the first high-precision structure study of the phase, Kalsbeek, Larsen, Rønsbo (1990) confirmed the long-suspected similarity of the britholite structure to the apatite structure. They proffered a same-cell  $P6_3$  apatite substructure for britholite, but they observed biaxial optics in one of the three britholite samples they studied [their “lessingite-(Ce)”, actually britholite-(Ce)], obviously incompatible with the reported hexagonal space group.

Recently, Hughes, Mariano, Drexler (1992) examined the atomic arrangement of synthetic samples of britholite-(La) and britholite-(Gd) and found the phases to crystallize as same-cell apatite substructures in space group  $P2_1$  (first setting for comparison to the hexagonal apatite structure). Their reported structure for monoclinic britholite is similar to that reported for the natural phase by Kalsbeek, Larsen, Rønsbo (1990), differing only in the ordering of long and short bonds from the apatite-equivalent Ca(1) sites to apatite O(3) equivalents.

We report here structure refinements of natural *monoclinic* britholite-(Ce) and britholite-(Y), performed before and after annealing to remove the effects of metamictization. The refinements demonstrate that both monoclinic and hexagonal dimorphs of the natural phase exist as a result of differing arrangements of long and short equivalents of the apatite Ca(1)-O(3) bonds, and resolve the long-standing paradox of britholite optical character.

## Experimental

Crystals of britholite-(Ce) from the Kipawa syenite gneiss complex and britholite-(Y) from Suishoyama, Japan (NSM-M17094, National Science Museum of Japan) were examined by optical and precession methods. Britholite-(Y) displayed a distinct non-zero  $2V$  angle under the polarizing microscope. The optical character of britholite-(Ce) was indeterminate because of the effects of metamictization. Complete precession suites were

obtained for both crystals to confirm the similarity with the apatite unit cell. Long-exposure photographs showed no evidence of the superstructure reflections present in  $P2_1/b$  apatite structures (Hughes, Cameron, Crowley, 1990). Sharp diffraction spots were evident for britholite-(Y), but diffractions for britholite-(Ce) were slightly diffuse, suggesting that the specimen was partially metamict, a common occurrence in britholite. The specimen was deemed suitable for preliminary structure determination, and data were collected on both britholite-(Ce) and britholite-(Y). Subsequent to solution and refinement of the structures, both phases were annealed by the method described by Mariano and Gower (1970). Data were then recollected, and the structures were refined on the intensity data from the annealed material.

A CAD4 diffractometer with graphite-monochromatized Mo radiation was used for crystal orientation and intensity data collection at 292 K. Unit cell parameters were obtained from refinement of the setting angles of 25 automatically-centered reflections. Other than unannealed britholite-(Ce), the  $\alpha$  and  $\beta$  unit cell parameters of all the phases refined to values within  $3\sigma$  of  $90^\circ$ ; those for britholite-(Ce) deviated from  $90^\circ$  by  $7\sigma$  and  $8\sigma$  for  $\alpha$  and  $\beta$ , respectively. Upon annealing the crystal the angles refined to essentially  $90^\circ$  (Table 1); we conclude that the deviation from  $90^\circ$  in  $\alpha$  and  $\beta$  in the unannealed phase results from the metamict nature of the crystal and not from triclinic symmetry. Crystal data, experimental conditions, and results of the refinement are given in Table 1.

### Structure refinement

All crystal structure calculations were undertaken using the SDP package of computer programs (Enraf-Nonius 1985). Data were reduced and corrected for Lorentz and polarization effects. Specimen absorption was corrected using psi scans, and subsequent to solution, theta-dependent corrections using the absorption-surface method as implemented in program *DIFABS* (Walker and Stuart, 1983).

Neutral atom scattering factors, with terms for anomalous dispersion, were taken from the International Tables for X-ray Crystallography (Vol. 4, 1974). Atomic parameters for the unannealed phases were obtained using a combination of direct methods (MULTAN-80; Main et al., 1980) and difference maps; the structures of the annealed phases were refined using the final atomic parameters of the respective unannealed phases. The structures were modeled in space group  $P2_1$ ; although *dimensionally* hexagonal, a previous study of "lessingite" [actually britholite-(Ce); Li, Wang and Liu, 1981] yielded that monoclinic space group, although the study was of rather low precision. In addition, the biaxial optics demand that the atomic arrangement crystallizes in a monoclinic or triclinic subsymmetry of the apatite  $P6_3/m$  space group. Allowable subsymmetries are  $P2_1/m$ ,  $P2_1$ ,  $Pm$ ,

**Table 1.** Crystal data, experimental conditions and the results of refinements for unannealed and annealed britholite-(Ce) and britholite-(Y).

	Britholite-(Ce)	Annealed Britholite-(Ce)	Britholite-(Y)	Annealed Britholite-(Y)
Crystal size (mm)	0.16 × 0.14 × 0.13	0.12 × 0.12 × 0.11	0.14 × 0.14 × 0.13	0.13 × 0.13 × 0.12
Space group	$P2_1$	$P2_1$	$P2_1$	$P2_1$
Unit Cell:				
Experimental				
<i>a</i>	9.580(5)	9.493(3)	9.422(1)	9.362(1)
<i>b</i>	9.590(4)	9.499(2)	9.414(2)	9.364(1)
<i>c</i>	6.980(3)	6.937(2)	6.7639(7)	6.731(1)
$\alpha$	90.22(3)	89.99(2)	90.02(1)	89.99(1)
$\beta$	89.69(4)	90.03(2)	89.992(9)	90.025(1)
$\gamma$	120.08(4)	120.04(2)	120.03(1)	120.01(1)
Refinement ( $P2_1$ )				
<i>a</i>	9.5804	9.4932	9.4216	9.3619
<i>b</i>	9.5901	9.4985	9.4138	9.3636
<i>c</i>	6.9802	6.9371	6.7639	6.7306
$\gamma$	120.079	120.038	120.0284	120.0121
Theta Range	0.1–30°	0.1–30°	1–30°	0.1–31°
Reflections	$\pm h \pm k + l$	$\pm h \pm k + l$	$\pm h \pm k + l$	$\pm h \pm k + l$
Scan time(s)	≤ 60	≤ 70	≤ 80	≤ 70
Scan type	0/20	0/20	0/20	0/20
Data collected	3506	3416	3264	3501
Unique data	1760	1714	1638	1755
$R_{merge}$	0.031	0.014	0.025	0.019
Reflections $l > 3\sigma_l$	543	1282	850	1090
Weights ( $w^{-1}$ )	$\sigma^2 F + 0.0016F^2$	$\sigma^2 F + 0.0016F^2$	$\sigma^2 F + 0.0016F^2$	$\sigma^2 F + 0.0001F^2$
<i>R</i>	0.048	0.018	0.034	0.025
$R_w$	0.046	0.026	0.036	0.023
$\Delta\rho$ residue ( $e^-/\text{\AA}^3$ )				
(+)	1.633	1.090	1.367	1.441
(–)	1.285	0.640	0.883	1.021

Note: Numbers in parentheses represent one *esd* of least units cited.

$P\bar{1}$  and  $P1$ . The  $N_z$  test for britholite-(Ce) was indeterminate; however, the  $N_z$  test for annealed britholite-(Ce), britholite-(Y), and annealed britholite-(Y) all yielded a decidedly acentric intensity distribution, allowing space groups  $P2_1$ ,  $Pm$ , and  $P1$ . All structures were successfully refined in space group  $P2_1$  (first setting) in accord with the studies of Li, Wang and Liu (1981) and Hughes, Mariano and Drexler (in press).

The structures were refined by minimizing  $\Sigma w(|F_o| - |F_c|)^2$  with  $l > 3\sigma_l$  data; an isotropic extinction factor was included in all refinements. Site

**Table 2.** Positional parameters and equivalent isotropic temperature factors ( $\text{\AA}^2$ ).

<b>REE(1a)</b>				
<i>unannealed Ce</i> (Ca <sub>0.19</sub> Ce <sub>0.81</sub> )	0.3335(4)	0.6671(4)	0.9860(7)	5.66(8)
<i>annealed Ce</i> (Ca <sub>0.58</sub> Ce <sub>0.42</sub> )	0.33306(8)	0.66670(8)	−0.0054(1)	1.17(1)*
<i>unannealed Y</i> (Y <sub>0.88</sub> Lu <sub>0.12</sub> )	0.3338(2)	0.6662(2)	0.0045(3)	2.63(3)*
<i>annealed Y</i> (Ca <sub>0.04</sub> Y <sub>0.96</sub> )	0.3330(1)	0.6666(1)	0.9854(2)	1.35(2)*
<b>REE(1b)</b>				
<i>unannealed Ce</i> (Ca <sub>0.71</sub> Ce <sub>0.29</sub> )	0.3329(3)	0.6664(3)	0.4884(6)	0.03(4)
<i>annealed Ce</i> (Ca <sub>0.63</sub> Ce <sub>0.37</sub> )	0.33361(8)	0.66653(8)	0.4934(1)	0.89(1)*
<i>unannealed Y</i> (Ca <sub>0.20</sub> Y <sub>0.80</sub> )	0.3329(2)	0.6670(2)	0.5078(3)	0.87(3)*
<i>annealed Y</i> (Ca <sub>0.19</sub> Y <sub>0.81</sub> )	0.3337(1)	0.6667(1)	0.4884(2)	0.70(2)*
<b>REE(2a)</b>				
<i>unannealed Ce</i> (Ca <sub>0.40</sub> Ce <sub>0.60</sub> )	0.9905(3)	0.2412(3)	0.244(2)	3.16(5)
<i>annealed Ce</i> (Ca <sub>0.40</sub> Ce <sub>0.60</sub> )	0.99015(5)	0.24053(5)	0.2437(4)	1.011(8)*
<i>unannealed Y</i> (Y <sub>0.93</sub> Lu <sub>0.07</sub> )	0.9947(1)	0.2422(1)	0.259(1)	1.79(2)*
<i>annealed Y</i> (Y <sub>0.96</sub> Lu <sub>0.04</sub> )	0.99496(7)	0.24204(8)	0.2359(6)	0.92(1)*
<b>REE(2b)</b>				
<i>unannealed Ce</i> (Ca <sub>0.42</sub> Ce <sub>0.58</sub> )	0.2407(3)	0.2501(3)	0.738(2)	3.13(5)
<i>annealed Ce</i> (Ca <sub>0.41</sub> Ce <sub>0.59</sub> )	0.24055(5)	0.25039(5)	0.7435(4)	1.022(8)*
<i>unannealed Y</i> (Y <sub>0.94</sub> Lu <sub>0.06</sub> )	0.2423(1)	0.2473(1)	0.757(1)	1.75(2)*
<i>annealed Y</i> (Y <sub>0.95</sub> Lu <sub>0.05</sub> )	0.24209(7)	0.24715(7)	0.7374(6)	0.98(1)*
<b>REE(2c)</b>				
<i>unannealed Ce</i> (Ca <sub>0.43</sub> Ce <sub>0.57</sub> )	0.2502(3)	0.0091(3)	0.233(2)	2.98(5)
<i>annealed Ce</i> (Ca <sub>0.41</sub> Ce <sub>0.59</sub> )	0.25040(5)	0.00989(5)	0.2445(4)	0.999(8)*
<i>unannealed Y</i> (Y <sub>0.93</sub> Lu <sub>0.07</sub> )	0.2473(1)	0.0050(1)	0.257(1)	1.85(2)*
<i>annealed Y</i> (Y <sub>0.95</sub> Lu <sub>0.05</sub> )	0.24711(8)	0.00505(7)	0.2381(6)	0.97(1)*

Table 2. (Continued)

<b>Si(1)</b>				
<i>unannealed Ce</i>	0.0256(9)	0.6287(9)	1/4	2.1(2)
<i>annealed Ce</i>	0.0284(2)	0.6296(2)	1/4	0.70(3)*
<i>unannealed Y</i>	0.0260(4)	0.6270(4)	1/4	1.01(5)
<i>annealed Y</i>	0.0265(2)	0.6282(2)	1/4	0.64(3)
<b>Si(2)</b>				
<i>unannealed Ce</i>	0.3712(9)	0.3980(9)	0.249(4)	2.2(2)
<i>annealed Ce</i>	0.3702(2)	0.3985(2)	0.243(1)	0.72(3)*
<i>unannealed Y</i>	0.3727(4)	0.3992(4)	0.274(1)	1.11(5)
<i>annealed Y</i>	0.3712(2)	0.3981(2)	0.2334(9)	0.60(3)
<b>Si(3)</b>				
<i>unannealed Ce</i>	0.6024(9)	0.9727(9)	0.248(4)	2.3(2)
<i>annealed Ce</i>	0.6012(2)	0.9715(2)	0.2407(9)	0.72(3)*
<i>unannealed Y</i>	0.6010(4)	0.9738(4)	0.250(1)	1.12(6)
<i>annealed Y</i>	0.6017(2)	0.9731(2)	0.234(1)	0.72(3)
<b>O(1a)</b>				
<i>unannealed Ce</i>	0.837(2)	0.511(2)	0.23(1)	3.4(5)
<i>annealed Ce</i>	0.8354(5)	0.5115(4)	0.236(2)	1.33(7)
<i>unannealed Y</i>	0.832(1)	0.507(1)	0.259(7)	2.4(2)
<i>annealed Y</i>	0.8320(6)	0.5074(6)	0.236(3)	1.8(1)
<b>O(1b)</b>				
<i>unannealed Ce</i>	0.489(2)	0.326(2)	0.223(7)	3.0(5)
<i>annealed Ce</i>	0.4878(5)	0.3230(5)	0.238(2)	1.40(7)
<i>unannealed Y</i>	0.491(1)	0.322(1)	0.275(5)	2.7(2)
<i>annealed Y</i>	0.4915(6)	0.3236(6)	0.251(3)	1.9(1)
<b>O(1c)</b>				
<i>unannealed Ce</i>	0.673(2)	0.165(2)	0.222(7)	2.8(5)
<i>annealed Ce</i>	0.6759(5)	0.1642(4)	0.253(2)	1.38(7)
<i>unannealed Y</i>	0.675(1)	0.169(1)	0.255(6)	2.4(2)
<i>annealed Y</i>	0.6762(6)	0.1686(6)	0.242(5)	2.0(1)
<b>O(2a)</b>				
<i>unannealed Ce</i>	0.405(2)	0.872(2)	0.269(4)	1.9(4)
<i>annealed Ce</i>	0.4056(5)	0.8739(4)	0.227(1)	1.20(7)
<i>unannealed Y</i>	0.403(1)	0.8704(9)	0.238(2)	1.6(2)
<i>annealed Y</i>	0.4026(6)	0.8719(6)	0.216(1)	0.9(1)
<b>O(2b)</b>				
<i>unannealed Ce</i>	0.466(2)	0.595(2)	0.252(9)	3.2(5)
<i>annealed Ce</i>	0.4681(4)	0.5945(4)	0.226(1)	0.97(7)
<i>unannealed Y</i>	0.468(1)	0.596(1)	0.236(2)	1.4(2)
<i>annealed Y</i>	0.4689(6)	0.5975(6)	0.217(1)	1.1(1)
<b>O(2c)</b>				
<i>unannealed Ce</i>	0.129(2)	0.534(2)	0.262(5)	2.5(4)
<i>annealed Ce</i>	0.1266(4)	0.5328(4)	0.267(1)	0.90(7)
<i>unannealed Y</i>	0.130(1)	0.5336(9)	0.288(2)	1.8(2)
<i>annealed Y</i>	0.1275(6)	0.5312(6)	0.271(1)	1.1(1)

Table 2. (Continued)

<b>O(3a)</b>				
<i>unannealed Ce</i>	0.635(2)	0.902(2)	0.043(4)	2.1(5)
<i>annealed Ce</i>	0.6392(5)	0.9010(5)	0.0538(9)	0.85(8)
<i>unannealed Y</i>	0.628(1)	0.896(1)	0.062(2)	1.8(2)
<i>annealed Y</i>	0.6378(7)	0.8998(7)	0.048(1)	1.2(1)
<b>O(3b)</b>				
<i>unannealed Ce</i>	0.692(3)	0.935(3)	0.410(6)	5.8(8)
<i>annealed Ce</i>	0.6828(6)	0.9237(6)	0.420(1)	1.5(1)
<i>unannealed Y</i>	0.686(1)	0.925(1)	0.442(2)	2.3(2)
<i>annealed Y</i>	0.6897(8)	0.9268(8)	0.420(1)	1.9(1)
<b>O(3c)</b>				
<i>unannealed Ce</i>	0.272(2)	0.370(2)	0.046(4)	2.2(5)
<i>annealed Ce</i>	0.2613(5)	0.3602(5)	0.0546(8)	0.86(8)
<i>unannealed Y</i>	0.266(1)	0.367(1)	0.061(2)	1.5(2)
<i>annealed Y</i>	0.2615(7)	0.3621(7)	0.046(1)	0.9(1)
<b>O(3d)</b>				
<i>unannealed Ce</i>	0.239(3)	0.309(3)	0.417(5)	4.0(6)
<i>annealed Ce</i>	0.2407(6)	0.3171(6)	0.421(1)	1.7(1)
<i>unannealed Y</i>	0.237(2)	0.310(1)	0.438(2)	3.1(3)
<i>annealed Y</i>	0.2366(8)	0.3095(8)	0.419(1)	1.9(2)
<b>O(3e)</b>				
<i>unannealed Ce</i>	0.067(3)	0.760(3)	0.068(5)	4.9(7)
<i>annealed Ce</i>	0.0762(6)	0.7581(6)	0.0706(9)	1.32(9)
<i>unannealed Y</i>	0.075(1)	0.761(1)	0.085(2)	2.3(2)
<i>annealed Y</i>	0.0731(8)	0.7632(8)	0.070(1)	1.8(1)
<b>O(3f)</b>				
<i>unannealed Ce</i>	0.100(2)	0.730(2)	0.436(4)	2.3(5)
<i>annealed Ce</i>	0.0999(6)	0.7380(5)	0.4395(9)	1.11(8)
<i>unannealed Y</i>	0.102(1)	0.733(1)	0.468(2)	1.9(2)
<i>annealed Y</i>	0.1013(7)	0.7386(6)	0.445(1)	0.8(1)
<b>F,OH</b>				
<i>unannealed Ce</i>	-0.001(4)	0.998(4)	0.191(5)	8.2(7)
<i>annealed Ce</i>	-0.0004(5)	0.9995(5)	0.2117(9)	2.18(8)
<i>unannealed Y</i>	0.000(2)	0.997(2)	0.231(3)	5.3(3)
<i>annealed Y</i>	0.0003(7)	0.0007(7)	0.212(1)	2.4(1)

\* Denotes equivalent isotropic displacement parameter for atoms refined with anisotropic displacement parameters.

occupancies of the REE sites were refined using Ca and Ce scattering factors for britholite-(Ce), and Ca and Y or Y and Lu for REE sites in britholite-(Y), depending on whether the mean Z of the site occupants was greater than or less than that of yttrium. Results of the site occupancy refinements are given in Table 2.

**Table 3.** Bond lengths of REE coordination polyhedra.

		Unannealed britho- lite-(Ce)	Annealed britho- lite-(Ce)	Unannealed britho- lite-(Y)	Annealed britho- lite-(Y)
<b>REE(1a)-</b>	O(1a)	2.42(7)	2.43(1)	2.30(3)	2.31(2)
	O(1b)	2.48(4)	2.43(1)	2.23(2)	2.25(2)
	O(1c)	2.47(4)	2.35(1)	2.33(3)	2.28(2)
	O(2a)	2.63(2)	2.366(7)	2.31(1)	2.298(6)
	O(2b)	2.53(5)	2.358(6)	2.30(1)	2.302(7)
	O(2c)	2.58(3)	2.558(6)	2.55(1)	2.561(7)
	O(3a)	2.66(2)	2.663(4)	2.552(9)	2.617(5)
	O(3c)	2.64(2)	2.670(5)	2.59(1)	2.614(6)
	O(3e)	3.15(4)	3.016(6)	3.03(2)	3.044(9)
<i>Mean</i>		2.6(1)	2.54(2)	2.47(6)	2.48(4)
<b>REE(1b)-</b>	O(1a)	2.39(7)	2.357(9)	2.33(3)	2.30(2)
	O(1b)	2.34(4)	2.37(1)	2.42(2)	2.38(2)
	O(1c)	2.31(4)	2.37(1)	2.31(3)	2.34(2)
	O(2a)	2.31(2)	2.530(7)	2.48(1)	2.496(7)
	O(2b)	2.39(5)	2.535(6)	2.51(1)	2.484(8)
	O(2c)	2.33(3)	2.332(6)	2.25(1)	2.243(6)
	O(3b)	3.14(2)	3.018(4)	3.011(9)	3.023(6)
	O(3d)	3.12(3)	3.020(6)	3.05(1)	3.032(7)
	O(3f)	2.62(3)	2.652(6)	2.56(1)	2.596(7)
<i>Mean</i>		2.6(1)	2.59(2)	2.55(5)	2.54(4)
<b>REE(2a)-</b>	O(1c)	2.75(2)	2.695(4)	2.73(1)	2.707(6)
	O(2c)	2.44(2)	2.410(4)	2.385(8)	2.359(5)
	O(3c)	2.71(2)	2.590(5)	2.59(1)	2.515(6)
	O(3d)	2.45(3)	2.442(6)	2.37(2)	2.365(8)
	O(3e)	2.33(4)	2.355(7)	2.30(1)	2.332(8)
	O(3f)	2.38(3)	2.324(7)	2.22(1)	2.201(7)
	F,O	2.40(4)	2.346(6)	2.34(2)	2.291(8)
<i>Mean oxy</i>		2.51(7)	2.47(1)	2.43(3)	2.41(2)
<b>REE(2b)-</b>	O(1a)	2.74(3)	2.697(5)	2.74(1)	2.713(7)
	O(2b)	2.44(2)	2.399(4)	2.371(8)	2.349(5)
	O(3a)	2.67(3)	2.597(6)	2.59(1)	2.518(8)
	O(3b)	2.49(4)	2.444(7)	2.40(2)	2.367(9)
	O(3c)	2.39(2)	2.362(6)	2.30(1)	2.303(7)
	O(3d)	2.31(3)	2.326(8)	2.24(2)	2.232(8)
	F,O	2.36(3)	2.337(4)	2.30(1)	2.302(5)
<i>Mean oxy</i>		2.51(7)	2.47(2)	2.44(3)	2.41(2)

Refinement results are given in Table 1, and atomic position and isotropic B values are given in Table 2; Table 3 lists selected bond lengths for the REE coordination polyhedra. Anisotropic thermal parameters and listings of observed and calculated structure factors have been deposited.<sup>1</sup>

Table 3. (Continued)

	Unannealed britholite-(Ce)	Annealed britholite-(Ce)	Unannealed britholite-(Y)	Annealed britholite-(Y)	
REE(2c)-	O(1b)	2.74(2)	2.686(3)	2.711(8)	2.704(4)
	O(2a)	2.44(2)	2.400(5)	2.38(1)	2.347(6)
	O(3a)	2.38(3)	2.352(6)	2.33(1)	2.309(8)
	O(3b)	2.32(4)	2.336(7)	2.23(1)	2.231(9)
	O(3e)	2.43(3)	2.439(5)	2.35(1)	2.317(7)
	O(3f)	2.72(2)	2.617(5)	2.64(1)	2.573(6)
	F,O	2.37(4)	2.344(6)	2.30(2)	2.297(8)
Mean oxy		2.51(7)	2.47(1)	2.44(3)	2.41(2)

Throughout this work, atom nomenclature is chosen to parallel that of the conventional  $P6_3/m$  apatite nomenclature, e.g., REE(1a) and REE(1b) are the  $P2_1$  equivalents of the single Ca(1) site in  $P6_3/m$  apatite; REE(2a), REE(2b), and REE(2c) are the three degenerate equivalents of the  $P6_3/m$  apatite Ca(2) site; and Si(1), Si(2), and Si(3) are the three equivalents of the single  $P6_3/m$  apatite tetrahedral site. The oxygen atoms, O(1a–c), O(2a–c), and O(3a–f), are named to correspond to  $P2_1$  equivalents of the  $P6_3/m$  apatite O(1), O(2), and O(3) atoms.

Subsequent to structure analysis, the individual crystals used in the refinements were chemically analyzed by electron microprobe. The results yielded: britholite-(Ce) =  $(\text{Ca}_{2.24}\text{La}_{0.17}\text{Ce}_{1.23}\text{Pr}_{0.17}\text{Nd}_{0.35}\text{Sm}_{0.04}\text{Eu}_{0.01}\text{Gd}_{0.15}\text{Dy}_{0.07}\text{Ho}_{0.05}\text{Er}_{0.04}\text{Y}_{0.69})\Sigma = 5.34\text{Si}_{2.79}\text{O}_{24}(\text{F}_{0.84}\text{OH}_{0.16})$ ; britholite-(Y) =  $(\text{Ca}_{1.24}\text{Fe}_{0.21}\text{Mn}_{0.49}\text{La}_{0.01}\text{Ce}_{0.09}\text{Pr}_{0.01}\text{Nd}_{0.10}\text{Sm}_{0.05}\text{Tb}_{0.01}\text{Dy}_{0.26}\text{Ho}_{0.09}\text{Er}_{0.12}\text{Y}_{2.27})\Sigma = 4.95(\text{P}_{0.13}\text{Si}_{2.93})\Sigma = 3.06\text{O}_{24}(\text{F}_{0.93}\text{OH}_{0.07})$ , both on the basis of 13 anions and  $(\text{F} + \text{OH}) = 1$ . Deviations from the ideal apatite formula stoichiometry are attributed to the large uncertainties involved with analysis of REEs by electron probe microanalysis.

### Structure description

As noted above, the atomic arrangements of monoclinic britholite-(Ce) and britholite-(Y) were determined on both natural and annealed samples. The structural principles underlying the difference between monoclinic and

<sup>1</sup> Material supplemental to this paper can be ordered by referring to no. CSD 56116, the names of the authors and citation of the paper at the Fachinformationszentrum Energie-Physik-Mathematik GmbH, D-76344 Eggenstein-Leopoldshafen, FRG.

**Table 3.** Bond lengths of REE coordination polyhedra.

		Unannealed britholite-(Ce)	Annealed britholite-(Ce)	Unannealed britholite-(Y)	Annealed britholite-(Y)
<b>REE(1a)-</b>	O(1a)	2.42(7)	2.43(1)	2.30(3)	2.31(2)
	O(1b)	2.48(4)	2.43(1)	2.23(2)	2.25(2)
	O(1c)	2.47(4)	2.35(1)	2.33(3)	2.28(2)
	O(2a)	2.63(2)	2.366(7)	2.31(1)	2.298(6)
	O(2b)	2.53(5)	2.358(6)	2.30(1)	2.302(7)
	O(2c)	2.58(3)	2.558(6)	2.55(1)	2.561(7)
	O(3a)	2.66(2)	2.663(4)	2.552(9)	2.617(5)
	O(3c)	2.64(2)	2.670(5)	2.59(1)	2.614(6)
	O(3e)	3.15(4)	3.016(6)	3.03(2)	3.044(9)
<i>Mean</i>		2.6(1)	2.54(2)	2.47(6)	2.48(4)
<b>REE(1b)-</b>	O(1a)	2.39(7)	2.357(9)	2.33(3)	2.30(2)
	O(1b)	2.34(4)	2.37(1)	2.42(2)	2.38(2)
	O(1c)	2.31(4)	2.37(1)	2.31(3)	2.34(2)
	O(2a)	2.31(2)	2.530(7)	2.48(1)	2.496(7)
	O(2b)	2.39(5)	2.535(6)	2.51(1)	2.484(8)
	O(2c)	2.33(3)	2.332(6)	2.25(1)	2.243(6)
	O(3b)	3.14(2)	3.018(4)	3.011(9)	3.023(6)
	O(3d)	3.12(3)	3.020(6)	3.05(1)	3.032(7)
	O(3f)	2.62(3)	2.652(6)	2.56(1)	2.596(7)
<i>Mean</i>		2.6(1)	2.59(2)	2.55(5)	2.54(4)
<b>REE(2a)-</b>	O(1c)	2.75(2)	2.695(4)	2.73(1)	2.707(6)
	O(2c)	2.44(2)	2.410(4)	2.385(8)	2.359(5)
	O(3c)	2.71(2)	2.590(5)	2.59(1)	2.515(6)
	O(3d)	2.45(3)	2.442(6)	2.37(2)	2.365(8)
	O(3e)	2.33(4)	2.355(7)	2.30(1)	2.332(8)
	O(3f)	2.38(3)	2.324(7)	2.22(1)	2.201(7)
	F,O	2.40(4)	2.346(6)	2.34(2)	2.291(8)
<i>Mean oxy</i>		2.51(7)	2.47(1)	2.43(3)	2.41(2)
<b>REE(2b)-</b>	O(1a)	2.74(3)	2.697(5)	2.74(1)	2.713(7)
	O(2b)	2.44(2)	2.399(4)	2.371(8)	2.349(5)
	O(3a)	2.67(3)	2.597(6)	2.59(1)	2.518(8)
	O(3b)	2.49(4)	2.444(7)	2.40(2)	2.367(9)
	O(3c)	2.39(2)	2.362(6)	2.30(1)	2.303(7)
	O(3d)	2.31(3)	2.326(8)	2.24(2)	2.232(8)
	F,O	2.36(3)	2.337(4)	2.30(1)	2.302(5)
<i>Mean oxy</i>		2.51(7)	2.47(2)	2.44(3)	2.41(2)

Refinement results are given in Table 1, and atomic position and isotropic B values are given in Table 2; Table 3 lists selected bond lengths for the REE coordination polyhedra. Anisotropic thermal parameters and listings of observed and calculated structure factors have been deposited.<sup>1</sup>

Table 3. (Continued)

	Unannealed britholite-(Ce)	Annealed britholite-(Ce)	Unannealed britholite-(Y)	Annealed britholite-(Y)	
REE(2c)-	O(1b)	2.74(2)	2.686(3)	2.711(8)	2.704(4)
	O(2a)	2.44(2)	2.400(5)	2.38(1)	2.347(6)
	O(3a)	2.38(3)	2.352(6)	2.33(1)	2.309(8)
	O(3b)	2.32(4)	2.336(7)	2.23(1)	2.231(9)
	O(3e)	2.43(3)	2.439(5)	2.35(1)	2.317(7)
	O(3f)	2.72(2)	2.617(5)	2.64(1)	2.573(6)
	F,O	2.37(4)	2.344(6)	2.30(2)	2.297(8)
Mean <i>oxy</i>		2.51(7)	2.47(1)	2.44(3)	2.41(2)

Throughout this work, atom nomenclature is chosen to parallel that of the conventional  $P6_3/m$  apatite nomenclature, e.g., REE(1a) and REE(1b) are the  $P2_1$  equivalents of the single Ca(1) site in  $P6_3/m$  apatite; REE(2a), REE(2b), and REE(2c) are the three degenerate equivalents of the  $P6_3/m$  apatite Ca(2) site; and Si(1), Si(2), and Si(3) are the three equivalents of the single  $P6_3/m$  apatite tetrahedral site. The oxygen atoms, O(1a–c), O(2a–c), and O(3a–f), are named to correspond to  $P2_1$  equivalents of the  $P6_3/m$  apatite O(1), O(2), and O(3) atoms.

Subsequent to structure analysis, the individual crystals used in the refinements were chemically analyzed by electron microprobe. The results yielded: britholite-(Ce) =  $(\text{Ca}_{2.24}\text{La}_{0.17}\text{Ce}_{1.23}\text{Pr}_{0.17}\text{Nd}_{0.35}\text{Sm}_{0.04}\text{Eu}_{0.01}\text{Gd}_{0.15}\text{Dy}_{0.07}\text{Ho}_{0.05}\text{Er}_{0.04}\text{Y}_{0.69})\Sigma = 5.34\text{Si}_{2.79}\text{O}_{24}(\text{F}_{0.84}\text{OH}_{0.16})$ ; britholite-(Y) =  $(\text{Ca}_{1.24}\text{Fe}_{0.21}\text{Mn}_{0.49}\text{La}_{0.01}\text{Ce}_{0.09}\text{Pr}_{0.01}\text{Nd}_{0.10}\text{Sm}_{0.05}\text{Tb}_{0.01}\text{Dy}_{0.26}\text{Ho}_{0.09}\text{Er}_{0.12}\text{Y}_{2.27})\Sigma = 4.95(\text{P}_{0.13}\text{Si}_{2.93})\Sigma = 3.06\text{O}_{24}(\text{F}_{0.93}\text{OH}_{0.07})$ , both on the basis of 13 anions and  $(\text{F} + \text{OH}) = 1$ . Deviations from the ideal apatite formula stoichiometry are attributed to the large uncertainties involved with analysis of REEs by electron probe microanalysis.

### Structure description

As noted above, the atomic arrangements of monoclinic britholite-(Ce) and britholite-(Y) were determined on both natural and annealed samples. The structural principles underlying the difference between monoclinic and

<sup>1</sup> Material supplemental to this paper can be ordered by referring to no. CSD 56116, the names of the authors and citation of the paper at the Fachinformationszentrum Energie-Physik-Mathematik GmbH, D-76344 Eggenstein-Leopoldshafen, FRG.

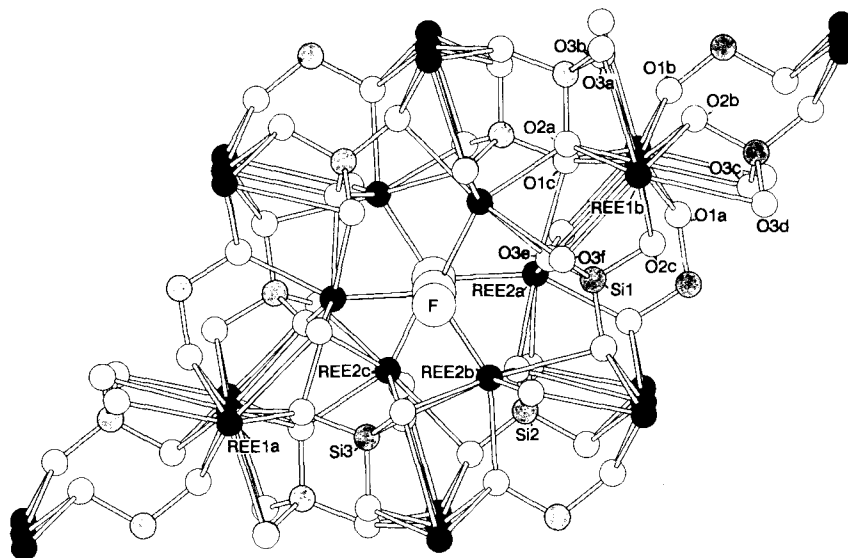


Fig. 1. Atomic arrangement of  $P2_1$  britholite tilted  $10^\circ$  from [001].

hexagonal britholite (Kalsbeek, Larsen and Rønsbo, 1990) were found to be the same in all the structures.

Like hexagonal britholite [all references to the hexagonal britholite structure refer to the work of Kalsbeek, Larsen and Rønsbo (1990)], the atomic arrangement of monoclinic britholite is similar to the apatite structure (Fig. 1). Despite substitution of elements widely disparate in size ([9]  $\text{Ca}^{2+} = 1.18 \text{ \AA}$ , [9]  $\text{Y}^{3+} = 1.075 \text{ \AA}$ , [9]  $\text{Ce}^{3+} = 1.196 \text{ \AA}$ ; [7]  $\text{Ca}^{2+} = 1.06 \text{ \AA}$ , [7]  $\text{Y}^{3+} = 0.96 \text{ \AA}$ , [7]  $\text{Ce}^{3+} = 1.07 \text{ \AA}$ ; Shannon, 1976) the fundamental apatite atomic arrangement remains intact in monoclinic britholite-(Ce) and britholite-(Y).

In  $P6_3/m$  apatite the tetrahedral sites are trigonally disposed about the [001] anion column; in  $P2_1$  britholite, the Si tetrahedra occupy essentially identical positions. For example, in natural britholite-(Ce) the Si(2) and Si(3) positions are within  $0.007 \text{ \AA}$  of the  $P6_3/m$  equivalents of Si(1) along  $a$ ,  $0.016 \text{ \AA}$  along  $b$ , and  $0.014 \text{ \AA}$  along  $c$ . Similarly, the positions of the degenerate  $P2_1$  equivalents of the single apatite Ca(2) site [REE(2a), REE(2b), and REE(2c)] deviate only slightly from  $P6_3/m$  equivalency; REE(2b) and REE(2c) positions deviate from  $P6_3/m$  equivalents of the REE(2a) site by less than  $0.005 \text{ \AA}$  along  $a$ ,  $0.004 \text{ \AA}$  along  $b$ , and  $0.08 \text{ \AA}$  along  $c$ . Finally among the cations, the degenerate equivalents of the apatite Ca(1) site [REE(1a) and REE(1b)] are within  $0.006 \text{ \AA}$  of  $P6_3/m$  equivalency along  $a$ ,  $0.007 \text{ \AA}$  along  $b$ , and  $0.18 \text{ \AA}$  along  $c$ . Thus, the cation positions are similar to those of the  $P6_3/m$  apatite structure. The monoclinic britholite

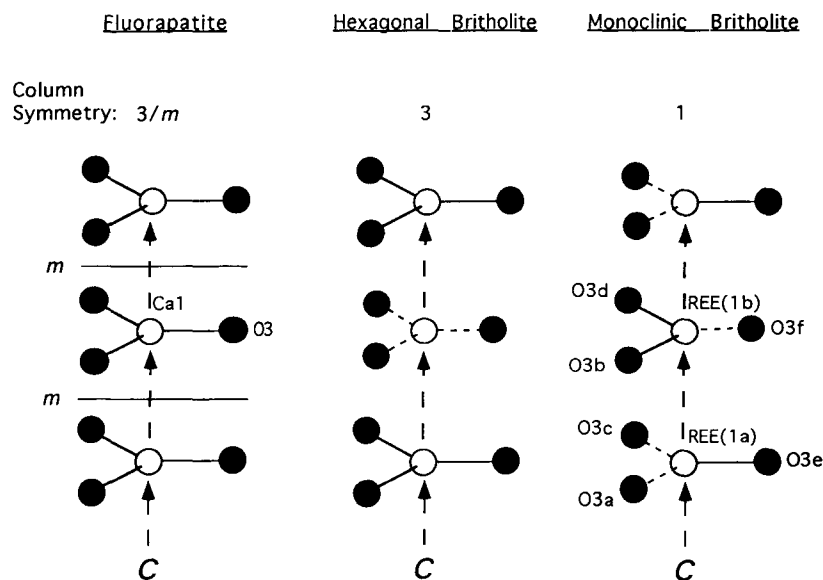


Fig. 2. Depiction of Ca(1)-O(3) triangles in apatite and REE(1)-O(3) triangles in britholite. In britholite structures, dashed bonds are short REE-O(3) bonds, and solid bonds are long REE-O(3) bonds. Arrangement of short and long bonds leads to  $P6_3$  symmetry in hexagonal britholite due to removal of  $m$  from symmetry elements, and  $P2_1$  symmetry in monoclinic britholite due to removal of  $3$  and  $m$  from symmetry elements.

atomic arrangement differs from the apatite atomic arrangement, however, principally in the positions of the O(3) atoms and concomitantly in the coordination polyhedra of atoms bonded to O(3).

In the  $P6_3/m$  apatite structure Ca(1) is bonded to three O(1) and three O(2) atoms in the form of a trigonal prism; Ca(1) is also bonded to an equilateral triangle of O(3) atoms through the prism faces, forming a tricapped trigonal prism. Each tricapped trigonal prism (site symmetry =  $3$ ) with its attendant O(3) triangle is related by (001) face-sharing to an adjacent Ca(1) polyhedron by mirror planes at  $z = 1/4, 3/4$ .

In  $P2_1$  britholite, the triad and the mirror planes are lost (removing  $3/m$  from the symmetry elements) as the O(3) atoms of (formerly) mirror-equivalent triangles shift in opposite directions (Fig. 2). The O(3) triangle bonded to the REE(1a) site has two O(3) atoms shifted towards that site [O(3a) and O(3c)] and one O(3) atom [O(3e)] shifted away from the site relative to the three equal bond lengths in  $P6_3/m$ ; the difference between long and short and long REE(1a)-O(3) bonds is approximately 0.36 Å in britholite-(Ce) and 0.42 Å in britholite-(Y), and the non-equivalence of the three bond-lengths destroys the three-fold axis. Conversely, the situation at the REE(1b) site is reversed as the O(3) atoms that would have been

related to O(3a) and O(3c) by a mirror plane [O(3b) and O(3d)] are shifted *away* from the Ca(1b) site whereas the O(3) atom formerly mirror-related to O(3e) [i.e., O(3f)] is shifted towards the Ca(1b) site. The REE(1a) site thus has *two short and one long* REE(1a)-O(3) bond(s), whereas the REE(1b) site has *two long and one short* REE(1b)-O(3) bond(s), removing 3/m from the symmetry elements.

The deviations of  $P6_3$  britholite from the  $P6_3/m$  apatite structure are similar to those of  $P2_1$  britholite, differing only in the “ordering” of long and short REE(1)-O(3) bonds (Fig. 2). In each britholite dimorph, three of the six “Ca(1)-O(3)” bonds that are equivalent in  $P6_3/m$  shorten in length, and the other three lengthen. In  $P6_3$  britholite, all three bonds to one Ca(1) equivalent lengthen, and all three bonds to the adjacent Ca(1) equivalent along [001] shorten; thus the triad is preserved but the mirror plane is removed from the symmetry elements, yielding space group  $P6_3$ .

## Discussion

The cause of the symmetry reduction from the apatite space group  $P6_3/m$  to britholite's  $P2_1$  may result from tetrahedral substitution and the increased bonding to the apatite-equivalent Ca(2) sites. The largest relative difference in radius between the substituents of apatite and britholite is in the tetrahedral site, with  $\text{Si}^{4+}$  (0.40 Å radius)  $\rightarrow$   $\text{P}^{5+}$  (0.31 Å radius). The more rigid  $\text{PO}_4$  tetrahedron in apatite allows little tetrahedral distortion; the less rigid  $\text{SiO}_4$  in britholite, however, allows shifts of O(3) atoms in response to a need for increased bonding in other sites.

Although *permitted* by the substitution of Si, the shift of O(3) atoms is interpreted as a mechanism to increase bonding in the Ca(1) and Ca(2) sites. The direction of offset between O(3) atoms indicates that for any pair of O(3) atoms bonded to the same Si (these are mirror equivalents in  $P6_3/m$  apatite), one of the O(3) atoms has shifted towards a Ca(2) site and the other has shifted towards a Ca(1) site. A comparison of tetrahedral angles in fluorapatite and britholite indicates that the positions of O(3) atoms in apatite tetrahedra lie between the O(3) positions of the britholite tetrahedra; this shows that O(3) positions in britholite have shifted in opposite directions from the O(3) position of apatite. One of the O(3) atoms bonded to a Si atom has shifted towards a Ca(2) site and away from a Ca(1) site, and the other has shifted towards a Ca(1) site and away from a Ca(2) site.

The *Distortion Theorem* of Brown and Shannon (1973) asserts that “in any coordination sphere in which the average bond length is kept constant, any deviation of the individual bond lengths from this value will increase the valence sum at the central atom”. In britholite, the “Ca(2)” sites are bonded to four O(3) atoms, two of which have been shifted towards this site and two of which have been shifted away from this site by an approxi-

mately equal distance. This shift of O(3) atoms relative to the calcium phosphate apatite structure leaves the mean REE(2a,b,c) bond lengths essentially constant and therefore increases bonding to the REE(2a,b,c) sites, in response to the substitution of REEs for Ca.

The differences between hexagonal britholite and monoclinic britholite result from differences in the ordering of the shifts of O(3) atoms (Fig. 2). For any pair of O(3) atoms bonded to the same Si atom, one of the O(3) atoms is always shifted toward a REE(1) site, and the other is shifted away from a REE(1) site; thus half of the REE(1)-O(3) bonds increase in length, and half are shortened. In the monoclinic dimorph each REE(1) atom has either two long bonds and one short [REE(1b)], or two short and one long [REE(1a)]. In the hexagonal dimorph, each REE(1) atom has either three long REE-O(3) bonds or three short REE-O(3) bonds. The different arrangement of O(3) shifts in the monoclinic and hexagonal dimorphs indicates that this ordering information is transmitted along the *c* axis and not perpendicular to it.

*Acknowledgements.* The U.S. National Science Foundation provided support for this project through grants EAR-8916305, (to JMH and Maryellen Cameron) and EAR-9218577 (to JMH).

## References

- Bøggild, O. B.: Om Britolitens Krystalform. *Medd. Grønl.* **47** (1911) 275–282.
- Brown, I. D., Shannon, R. D.: Empirical bond-strength-bond-length curves for oxides. *Acta Crystallogr.* **A29** (1973) 266–282.
- Enraf-Nonius: Structure determination package. Enraf-Nonius. Delft (1985).
- Gay, P.: An X-ray investigation of some rare-earth silicates: cerite, lessingite, britholite, beckelite, and stilwellite. *Mineral. Mag.* **31** (1957) 455–468.
- Genkina, E. A., Malinovskii, Y. A., Khomyakov, A. P.: Crystal structure of Sr-containing britholite. *Kristallografiya* **36** (1991) 39–43.
- Hata, S.: Abukumalite, a new mineral from pegmatites of Iisaka, Fukushima prefecture. *Sci. Pap. Inst. Phys. Chem. Res., Tokyo* **34** (1938) 1018–1023.
- Hughes, J. M., Cameron, M., Crowley, K. D.: Crystal structures of natural ternary apatites: solid solution in the  $\text{Ca}_5(\text{PO}_4)_3\text{X}$  ( $\text{X} = \text{F}, \text{OH}, \text{Cl}$ ) system. *Am. Mineral.* **75** (1990) 295–304.
- Hughes, J. M., Mariano, A. N., Drexler, J. W.: Crystal structures of synthetic Na-REE-Si oxyapatites, synthetic monoclinic britholite. *N. Jahrb. Mineral.*, in press (1992).
- Hughson, M. R., Sen Gupta, J. G.: A thorium intermediate member of the britholite-apatite series. *Am. Mineral.* **49** (1964) 937–951.
- International Tables for X-ray Crystallography. Vol. 4*, Birmingham, England: The Kynoch Press (1974).
- Kalsbeek, N., Larsen, S., Rønsbo, J. G.: Crystal structures of rare earth elements rich apatite analogues. *Z. Kristallogr.* **191** (1990) 249–263.
- Kupriyanova, I. I., Sidorenko, G. A.: Minerals of the britholite group. *Dokl. Akad. Nauk, SSSR* **148** (1963) 912–915.
- Li, D., Wang, P., Liu, J.: The crystal structure of lessingite, rich in light rare earth, cerium. *J. Chinese Silicate Soc.* **9** (1981) 422–432.
- Main, P., Fiske, S. J., Hull, S. E., Lessinger, L., Germaine, G., Declercq, J. O., Woolfson, M. M.: MULTAN-8. A system of computer programs for the automatic solution of

- crystal structures from X-ray diffraction data. (1980) Universities of York, England, and Louvain, Belgium.
- Mariano, A. N., Gower, J. A.: Eu geochemistry and its particular occurrence in the britholite zone, Oka, Quebec. Technical Report C-244, Ledgemont Laboratories, Kennecott Copper Company (1970).
- Shannon, R. D.: Revised effective ionic radii and systematic studies of interatomic distances in halides and chalcogenides. *Acta Crystallogr.* **A32** (1976) 751–767.
- Walker, N., Stuart, D.: An empirical method for correcting diffractometer data for absorption effects. *Acta Crystallogr.* **A39** (1983) 158–166.
- Winther, C.: Britholith, a new mineral. *Medd. Grønland.* **24** (1901) 190–196.